

Mixed-mode fracture (K_I and K_{II}) evaluation in epoxy resin using ASEN B configuration

Asymmetric Single Edge Notched Bend (ASENB) specimen which is exposed to asymmetric 3-point bending is used to estimate the mixed-mode fracture (I/II) in epoxy. The mode I and mode II combination stress intensity factors (SIF) were calculated for various locations of loading points and different crack lengths using the finite element analysis tool ANSYS. By selecting suitable points for the support positions with the loading point mode I to mode II mixities can be achieved. Then, several fracture tests on epoxy resin were conducted using the suggested ASEN B specimen. The crack path follows a straight line for mode I fracture and a curved path from the crack initiation angle for mode II fracture and mode II dominant loading. The broken specimen surfaces under various conditions of loading were observed using scanning electron microscopy (SEM). Fractured specimen surfaces of the tested specimens showed reasonably smooth patterns indicating cleavage fracture.

Keywords: Epoxy resin, fracture toughness, asymmetric single edge notched bend (ASENB) specimen, stress intensity factor (SIF), 3-point bending

1.0 Introduction

The manufacturing sector includes processes like casting, machining, forming, molding as the major parameters. In the above-said processes, we come across many defects in the finished products due to improper methods of manufacturing which are found in metal structures. All these defects are not so effective if they are serviced in time. Here comes the concept of fracture mechanics which deals with the finding of defects in the metal structure in terms of a crack. Fracture mechanics divides the cracks into two categories in which include the crack that will grow and affect the structure of the material and the safe crack (that will not grow further). With all these defects it is

still possible to have a safe operating condition through damage tolerance analysis.

Several engineering materials such as glasses, polymers, ceramics, and rocks made cracked components fail frequently due to brittle fracture. Precise interpretation for crack behaviour can be given by LEFM when there is negligible plastic deformation present in the vicinity of the crack tip. The occurrence of pre-existing cracks in the components and structures made of glass, ceramics, and polymers like brittle materials will undergo a catastrophic failure due to fracture. In many applications like aerospace, shipbuilding, etc. brittle materials were used. The main cause for failure of various brittle materials is the mixed-mode fracture i.e. mode I (opening) and mode II (sliding) combination.

Laboratory specimens are preferred by many researchers to investigate fracture behaviours as the experiments on real components are difficult and expensive. Many investigators investigated mixed-mode I/II fracture on PMMA e.g. [1], [2] and [3]. Epoxy and PMMA materials have been recognized for studying brittle fractures. The basic advantages of epoxy and PMMA materials during brittle fracture analysis include ease of manufacture, geometry and loading conditions, and the ability to generate complete fracture modes (Mode-I and Mode-II).

A semi-circular disk containing an edge crack loaded under 3-point bending is used for testing the mixed-mode fracture in PMMA is reported in [1], [2] and [3]. The semi-circular bend (SCB) configuration has newly acquired much consideration by investigators for testing opening mode (mode I) fracture strength of geo-materials and rocks [4]. The fracture strength measured with SCB specimens in opening mode is lower than level I and II values measured with CB specimens [5]. Edge cracked semi-circular disk (ECSD) specimens made of epoxy resin are used in [6] and [7] for fracture investigations. [8] Presents a test set-up using semi-circular bend (SCB) specimen for evaluating pure mode-II fracture toughness of asphalt concretes. [9] Showed that ECSD is ideal for fracture strength testing of ceramics and other brittle polymers under compression.

Mr. Shashidhara L C, Dayananda Sagar University Dr. Srinivas H K, SJB Institute of Technology, Dr. C. Anil Kumar, Sri Sai Ram College of Engineering, Dr. K. S. Narayanaswamy, Reva University and Dr. H. R. Vitala, SJB Institute of Technology, Bengaluru, India E-mail: shashidhar.lc@gmail.com / hksri2006@gmail.com / narayanswamys@gmail.com / canilkumarrichitha@gmail.com / vitala.hr@gmail.com

2.0 Nomenclature (Table 1)

TABLE 1: NOMENCLATURE

Symbol	Description	Unit
K	Stress intensity factor (SIF)	MPa√m
Y_I & Y_{II}	Geometric factor for mode-I and mode-II	
K_I & K_{II}	SIF for mode-I and mode-II	MPa√m
P_{cr}	Fracture load or critical load at the fracture	N
E	Young's modulus	Mpa
μ	Poison's ratio	
L	Length of specimen	mm
a	Crack length	mm
w	Width of specimen	mm
B	Thickness of specimen	mm
S_1 & S_2	Support location from the center of specimen	mm
a/W	Crack to width ratio	
ASENB	Asymmetric single edge notched bend specimen	
σ	Applied stress	N/mm ²
P	Applied load	N
LEFM	Linear elastic fracture mechanics	
ASTM	American society for testing and materials	

3.0 Test specimen configuration

In this investigation, Asymmetric Single Edge Notched Bend (ASENB) configuration is employed to study the mixed-mode (K_I and K_{II}) fracture. The single edge notched bend specimen with edge crack is subjected to three-point bend loading. The specimen is controlled by producing the specimens with a pre-defined edge crack to study the mixed-mode (K_I and K_{II}) relative combinations. The test configuration and condition of loading under the 3-point bend fixture are as shown in Figs.1 and 2. The test configuration of the specimen is containing a sharp edge notch of length 'a' along the symmetric line of width and length 'L' is loaded symmetrically for pure mode I and asymmetrically for mixed-mode and pure mode II using a universal testing machine.

Opening mode fracture state is studied by keeping the

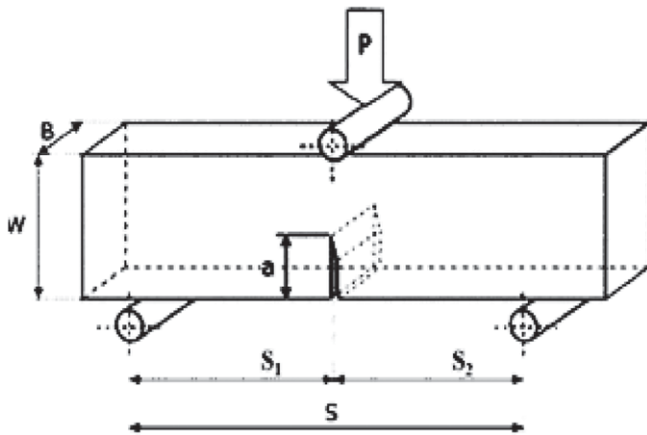


Fig.1: Standard ASENb specimen configuration for pure mode I fracture

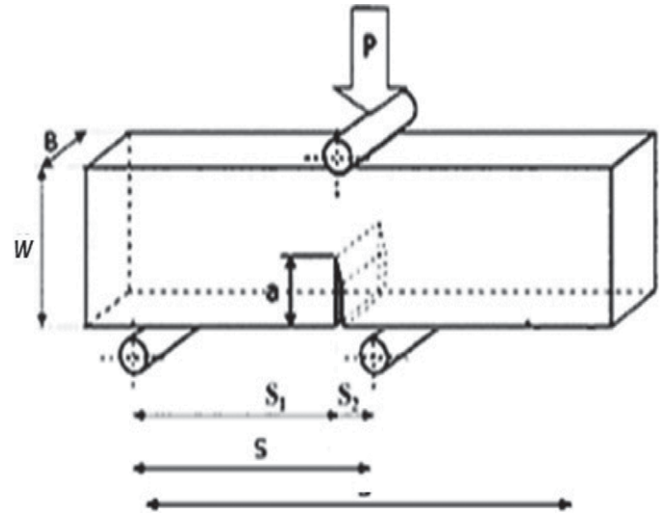


Fig.2: Standard ASENb specimen configuration for pure mode II fracture

distance between the bottom support as same i.e. ($S_1=S_2$) and one of the bottom support locations (S_2) is kept near to the crack front to study the sliding mode fracture. In this experimental investigation to study how the fracture toughness transforms from opening mode to sliding mode fracture over different mixed modes the support location (S_1) is kept constant and (S_2) is varied to obtain the mixed-mode fracture states. By varying the gap between two support locations the mixed-mode states can be controlled to find the effect of both fracture modes I and II.

4.0 Numerical analysis

The supports with their loading locations are S_1 and S_2 and the crack length is given as 'a'. These two parameters are the functions of SIF namely K_I and K_{II} for the specimen. The SIF for different values of S_2 is obtained by using the post-processing command KCALC in ANSYS. The geometric factors Y_I and Y_{II} are obtained from the below equations.

$$K_I = \frac{P}{2wB} \sqrt{\pi a} Y_I(a/w, S_1/w, S_2/w) \quad \dots (1)$$

$$K_{II} = \frac{P}{2wB} \sqrt{\pi a} Y_{II}(a/w, S_1/w, S_2/w) \quad \dots (2)$$

Where, σ_0 denotes to applied stress and Y_I and Y_{II} are respective geometry factors in mode I and mode II fracture. Evaluation of stress intensity factor using SCB specimens through ANSYS is presented earlier in [10]. Various ASENb specimen models were evaluated using ANSYS to find Y_I and Y_{II} . The following are the loading conditions considered for the geometry: $W=20$, $B=10$, $P=100$ N. S_1 was set to a fixed value of 40 mm and S_2 varied between 6.07 and 40 mm to adjust the state of the mixed-mode. In the finite element models, the elastic material properties of epoxy resin given in Table 2 were also considered. Figs.3 and 4 show a typical finite element model of the ASENb specimen and triangular elements at the crack tip singularity respectively. At the

vicinity of the crack tip, isoparametric singular triangular (STRIA 6) elements are used and a compatible mesh of quadrilateral elements quadratic in order with 8 nodes (QUAD 8) in the rest of the domain is used. Figs.1 and 2 indicate a 100 N point load applied at the top. Support point nodes are constrained in the Y direction.

TABLE 2: SPECIMEN DIMENSIONS AND MATERIAL PROPERTIES

Specimen dimensions	L=120mm, $S_1=40\text{mm}$, $S_2=6.07\text{mm}$ to 40mm a=10mm, B=10mm, w=20mm
Material properties of epoxy	E=3Gpa, $\mu=0.33$

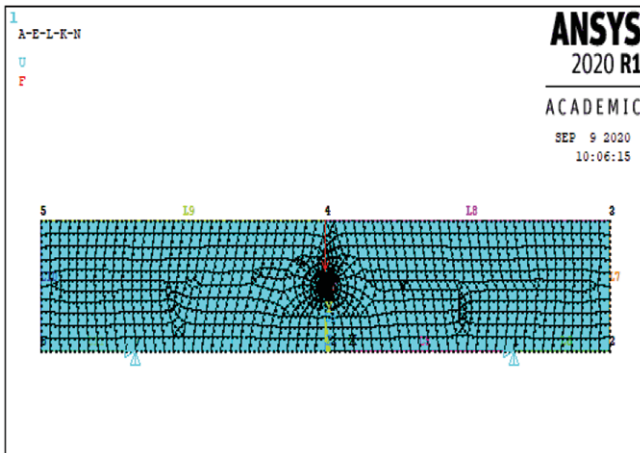


Fig.3: The finite element model of ASEN specimen

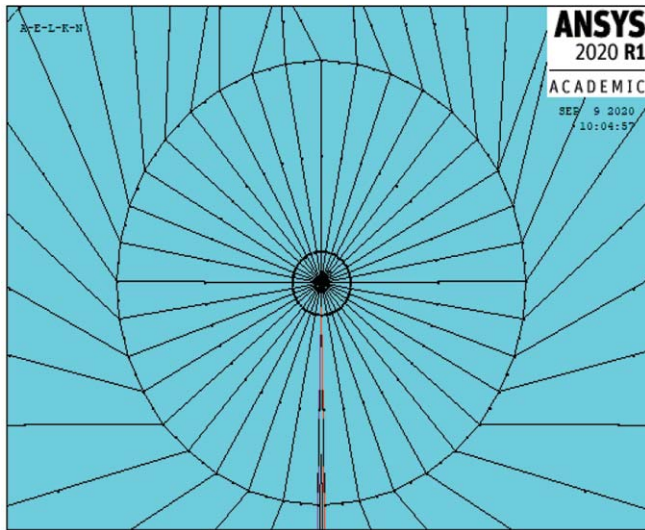


Fig.4: Triangular elements at the crack tip singularity

Von mises equivalent stress contour plots for pure mode I and pure mode II loading are captured using ANSYS graphical post-processing capabilities are shown in Figs.5 and 6 respectively. Von mises equivalent stress contour plots near the crack tip for mode I and mode II loading are shown in Figs.7 and 8 respectively. Fig.9 shows the transformation of contour plot shapes near the crack tip from pure mode I to pure mode II when supporting location S2 near to the crack plane.

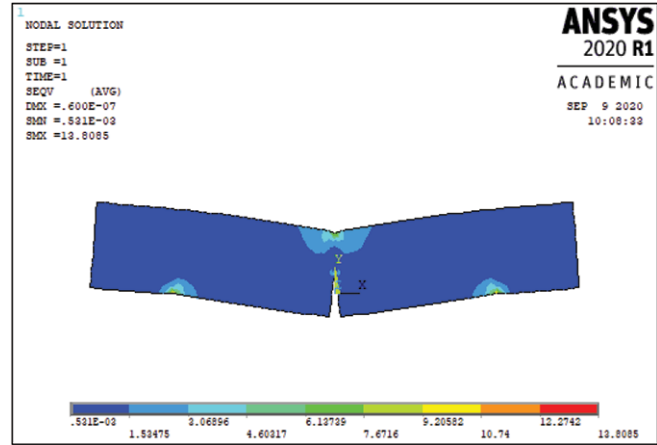


Fig.5: Von mises stress plot for pure mode-I loading

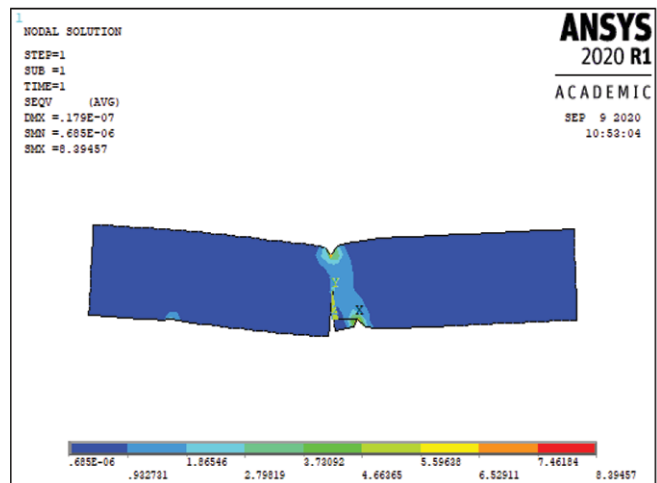


Fig.6: Von mises stress plot for pure mode-II loading

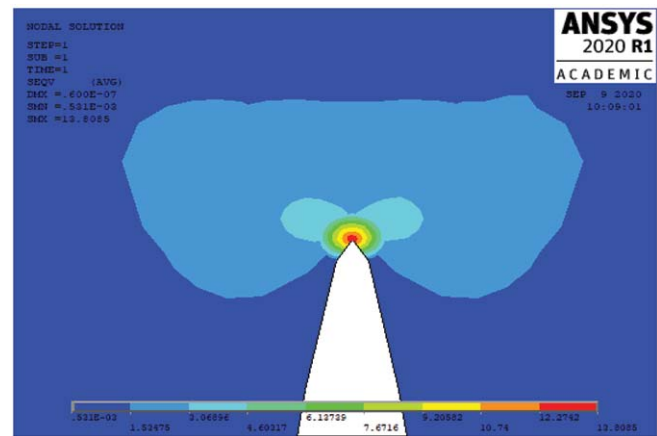


Fig.7: Contour plot at the crack tip for pure mode-I loading

5.0 Experimental analysis

Several mixed-mode fracture tests are carried out on epoxy resin to study the experimental applicability of the ASEN configuration. From an epoxy sheet of 10 mm thickness, 25 specimens were fabricated. The sizes of specimens are selected as per the ASTM standard. Width of the specimen

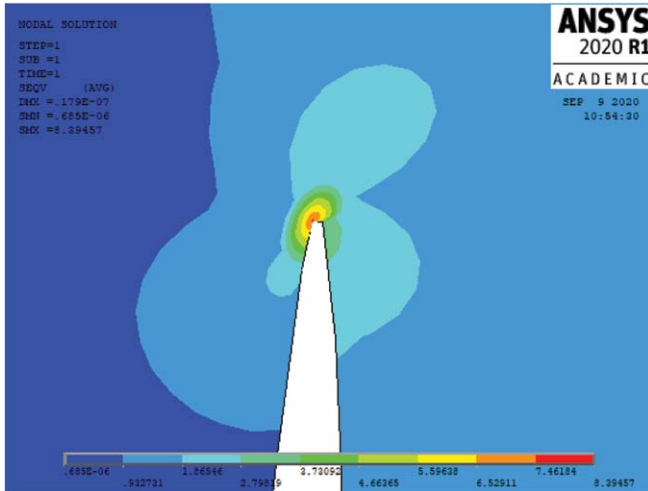


Fig.8: Contour plot at the crack tip for pure mode-II loading

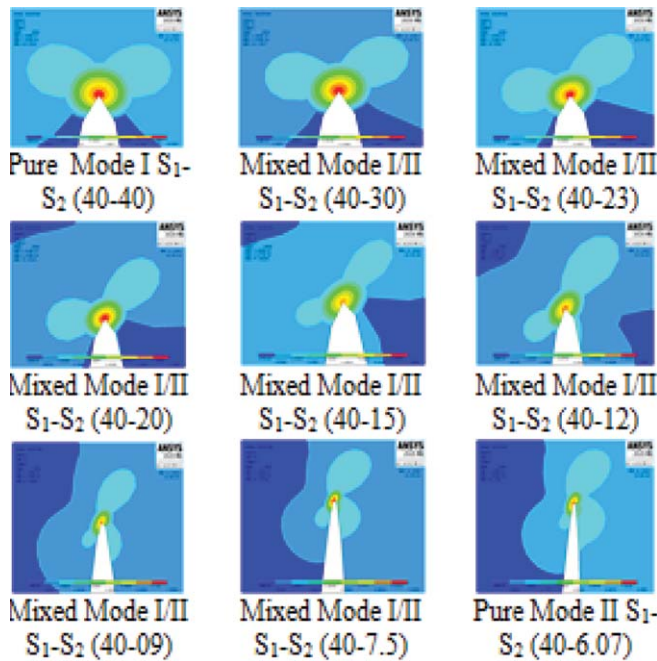


Fig.9: Transformation of contour plot shapes near the crack tip from pure mode I to pure mode II

$W=20$ mm, notch length $a=10$ mm and thickness $B=10$ mm. The notch length to width ratio a/W was taken as 0.5 in the test samples. A very thin fret saw blade of 0.4 mm thickness was used to create a notch with an initial depth of slightly less than 7.5 mm. Then by pressing a razor blade sensibly a sharp pre-crack equal to 10 mm was created.

For all the tests the support location S_1 was set equal to 40 mm and then the full variety of mixed-mode I/II cases was covered by considering the S_2 values in mm $S_2=\{40$ (pure mode I), 25, 18, 15, 12, 10 (mode mixities) and 8 (pure mode II)}. A minimum of three specimens was prepared for each mode mixities. Then each specimen is loaded on INSTRON 5582 UTM of 150 kN capacity using the 3 point bend fixture

with chosen S_1 and S_2 values as shown in Figs.10 and 11. And 0.5 mm/min constant load rate is maintained until the final fracture. During the test, the load-displacement data were recorded.

6.0 Result presentation

6.1 FINITE ELEMENT EVALUATION

The SIF for different values of S_2 and a/W are calculated using the post-processing command KCALC in ANSYS. The corresponding normalized SIF (geometric factors) Y_I and Y_{II} are obtained from equations 1 and 2. The results are presented in Table 3.

Figs.12 and 13 show mode I and mode II geometry factors (Y_I and Y_{II}) variation against support location (S_2) to width (w) ratio (S_2/w) respectively. The mode-I geometry factor Y_I

TABLE 3: NORMALIZED SIF FOR DIFFERENT VALUES OF S_2/w

Crack length to width ratio $a/w=0.25$				
S_2/w	K_I	K_{II}	Y_I	Y_{II}
2	5.5455	0	5.5982	0
1.5	4.6101	0.12902	4.6539	0.1302
1.15	3.7971	0.23533	3.8332	0.2375
1	3.3855	0.28576	3.4176	0.2884
0.75	2.385	0.43891	2.4076	0.443
0.6	2.0588	0.4834	2.0783	0.4879
0.45	1.3995	0.65331	1.4128	0.6595
0.375	0.8227	0.91774	0.8305	0.9264
0.3035	0	1.0577	0	1.0677
Crack length to width ratio $a/w=0.35$				
S_2/w	K_I	K_{II}	Y_I	Y_{II}
2	5.6066	0	4.7834	0
1.5	4.5764	0.1967	3.9045	0.1678
1.15	3.7104	0.3636	3.1656	0.31022
1	3.2711	0.4439	2.7908	0.3787
0.75	2.1976	0.5923	1.8749	0.5053
0.6	1.6216	0.7664	1.3835	0.6539
0.45	1.2866	1.0293	1.0977	0.8781
0.375	0.8181	1.2058	0.698	1.0287
0.3035	0	1.4495	0	1.2367
Crack length to width ratio $a/w = 0.5$				
S_2/w	K_I	K_{II}	Y_I	Y_{II}
2	5.4104	0	3.8621	0
1.5	4.2683	0.2877	3.0468	0.2053
1.15	3.3601	0.5107	2.3985	0.3645
1	2.9141	0.6205	2.0802	0.4429
0.75	2.0881	0.8473	1.4905	0.6048
0.6	1.5157	1.0508	1.0819	0.7501
0.45	0.8299	1.3919	0.5924	0.9936
0.375	0.4431	1.653	0.3163	1.1799
0.3035	0	2.0391	0	1.4556



Fig.10: Specimen loaded on Instron 5582 UTM

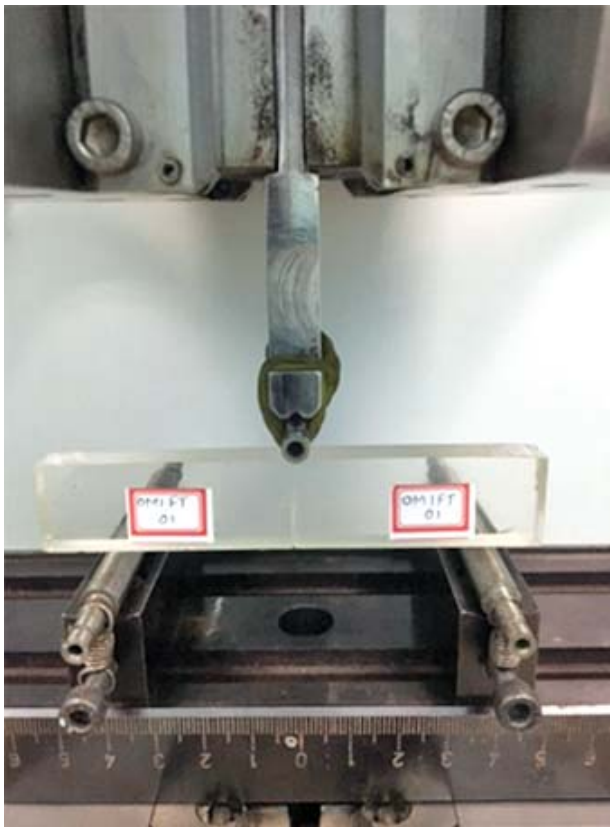


Fig.11: Specimen loaded on three-point bend fixture [Courtesy: National Aeronautical Laboratory (NAL)]

decreases in all the a/w values as the support location S_2 moves closer to the crack plane (varies between $40 e'' S_2 e'' 6.07$). And increased values of geometry factor Y_I can be observed when the crack length to width ratio a/w decreases from 0.5 to 0.25. Similarly, the mode-II geometry factor Y_{II} increases as the support location S_2 (varies between $40 e'' S_2 e'' 6.07$) moves closer to the crack plane for all the a/w values. And decreased values of geometry factor Y_{II} can be observed when the crack length to width ratio a/w decreases from 0.5 to 0.25. The SIF solutions for the problem on hand achieved using Abaqus software are also reported in [1]. It is gratifying to note a close agreement between the two.

6.2 TENSILE TEST

A tensile test experiment is carried out to find the modulus of elasticity 'E' and ultimate tensile strength of the fabricated epoxy specimens before undergoing finite element evaluation and the fracture toughness tests. The results obtained in the test are tabulated in Table 4. The stress-strain diagram obtained from the tension tests 1, 2, and 3 are shown in Figs.14, 15, and 16 respectively.

TABLE 4: TENSILE TEST RESULTS ON EPOXY SPECIMENS

Findings	Test-1	Test-2	Test-3	Average result
Initial area in mm ²	96.87	97.84	98.87	97.86
Initial gauge length in mm	50	50	50	50
Final gauge length in mm	51.74	51.84	51.97	51.85
Yield strength in MPa	97.32	98.57	96.58	97.49
Ultimate tensile load in KN	9.11	10.12	10.07	9.77
Ultimate tensile strength in MPa	102.32	103.47	101.87	102.55
% Elongation	3.48	3.68	3.94	3.7

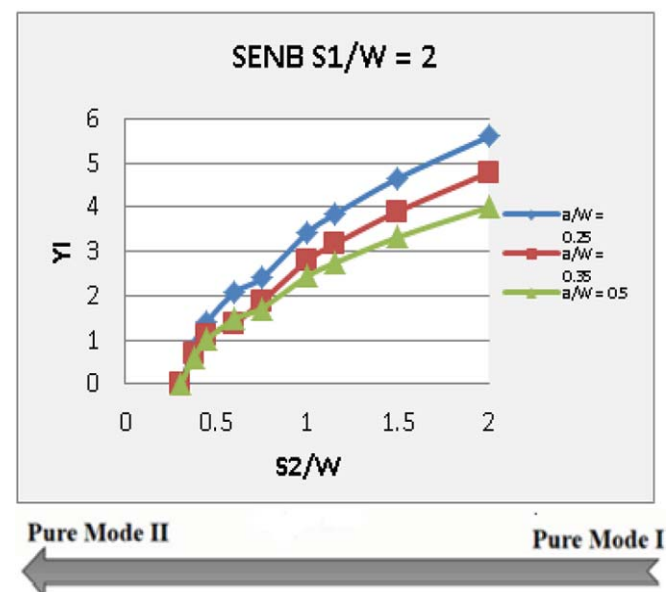


Fig.12: Variation of mode-I geometry factor vs S_2/W

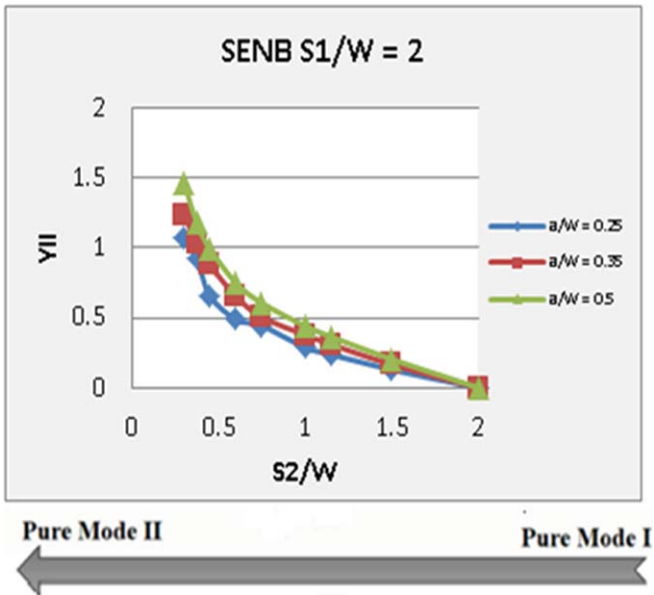


Fig.13: Variation of mode-II geometry factor vs S_2/W

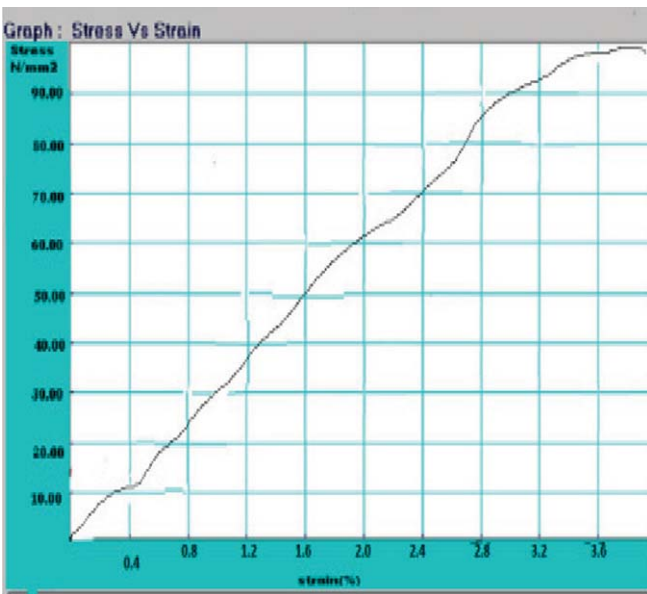


Fig.14: Stress-strain diagram obtained in test-1

6.3 FRACTURE TOUGHNESS TEST

Several fracture tests are carried out on proposed ASENb configurations made of epoxy resin to evaluate the mixed-mode fracture behaviour. Figs.17 and 18 depict the fracture paths discovered for the tested specimens under various combinations of mode I and mode II. As the support locations, S_2 moves closer to the crack plane the fracture load (P_{cr}) increases due to the increased resistance offered by the material. Material resistance has increased particularly for mode II dominant loading conditions and variation of fracture load vs different support locations as shown in Fig.19. The summary of the fracture load (P_{cr}) obtained during mixed-mode fracture toughness tests conducted on different ASENb

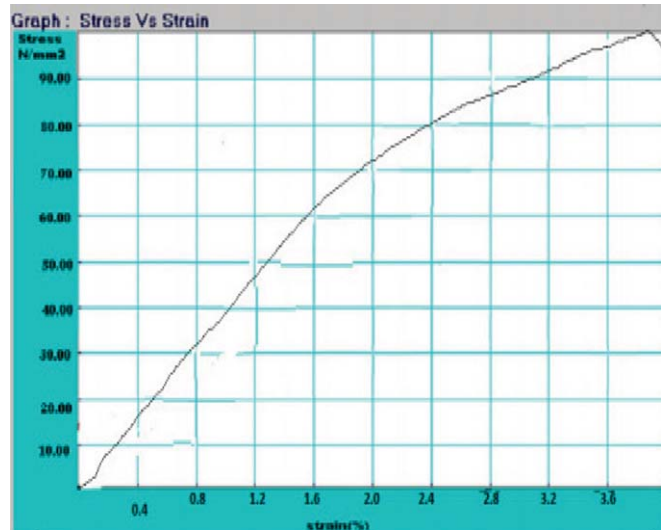


Fig.15: Stress-strain diagram obtained in test-2

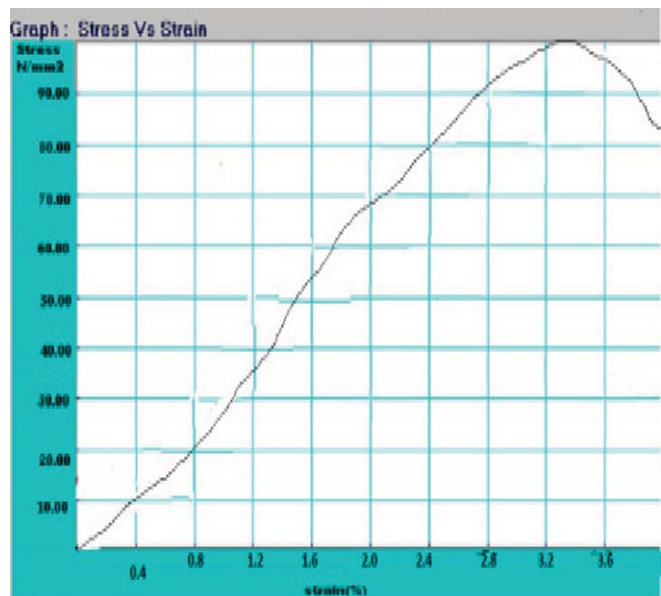


Fig.16: Stress-strain diagram obtained in test-3

specimen configurations prepared by epoxy resin is listed in the Table 5.

6.4 MICROSTRUCTURE STUDY

Studying the appearances of the fractured surface can help to define the cause of failure in an engineered product. Different modes of fracture failure yield characteristic feature on the surface, permitting a scientific analysis to determine the root cause of the failure. Fractured ASENb specimens are observed under a scanning electron microscope to study the microstructural changes during the brittle fracture of epoxy material. Considerable details about the cause of the fracture and the mechanisms of damage may be acquired from a thorough analysis of the surfaces of the fracture. Examination of fractured epoxy surfaces highlights the occurrence of

TABLE 5: SUMMARY OF THE RESULTS OBTAINED FROM MIXED MODE I/II FRACTURE TESTS CONDUCTED ON ASENb SPECIMENS MADE OF EPOXY RESIN. (Specimen code X-Y-Z: X=S1 (mm), Y=S2 (mm), Z=test number)

	Specimen code	Pcr (kN)	KI (MPa√m)	KII (MPa√m)
1	40-40-1 (mode I)	241.23	13.05	0.00
2	40-40-2 (mode I)	334.37	18.10	0.00
3	40-40-3 (mode I)	217.18	11.75	0.00
4	40-40-4 (mode I)	235.16	12.73	0.00
5	40-25-1	549.16	18.46	2.81
6	40-25-2	431.39	14.50	2.20
7	40-25-3	314.02	10.55	1.60
8	40-18-1	428.74	12.50	2.66
9	40-18-2	439.23	12.80	2.73
10	40-18-3	461.37	13.45	2.86
11	40-15-1	634.37	13.25	5.38
12	40-15-2	604.19	12.62	5.12
13	40-15-3	668.11	13.95	5.66
14	40-12-1	557.59	8.45	5.86
15	40-12-2	560.66	8.50	5.89
16	40-12-3	690.36	10.47	7.26
17	40-12-4	822.18	12.46	8.64
18	40-10-1	1051.47	8.73	14.64
19	40-10-2	822.74	6.83	11.45
20	40-10-3	922.09	7.66	12.84
21	40-10-4	964.75	8.01	13.43
22	40-8-1 (mode II)	1021.78	0.00	16.89
23	40-8-2 (mode II)	1234.85	0.00	20.42
24	40-8-3 (mode II)	1269.71	0.00	20.99
25	40-8-4 (mode II)	1570.54	0.00	25.97

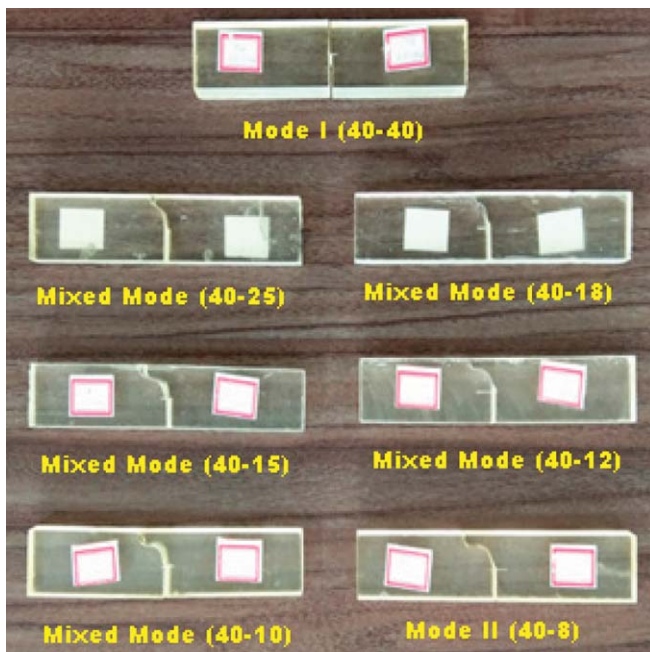


Fig.17: Fractured specimens under mode I to mode II loading



Fig.18: Other fractured ASENb test specimens

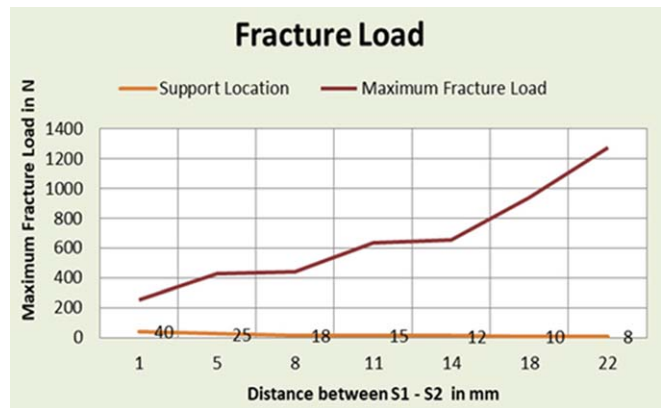


Fig.19: Variation of fracture load vs different support locations

cleavage fracture. Fractured specimen surfaces of the tested specimens showed reasonably smooth patterns as shown in Figs.20(a) and 20(b). Because of the rapid early crack progression, the crack surface near this initiation region is moderately smooth. And with further amplification, surfaces seemed slightly coarser indicating the transition zone as shown in Figs.20(c) and 20(d). With greater magnification Figs.20(e) and 20(f) shows the striation marks resembling flow marks successively in the path of crack propagation. The occurrence of striations in distinction to a glassy surface shows more energy absorption.

7.0 Conclusions

In this analysis, the ANSYS programme is used to calculate exact mixed-mode SIF solutions for an ASENb specimen. The test configuration for mixed-mode (K_I and K_{II}) fracture tests

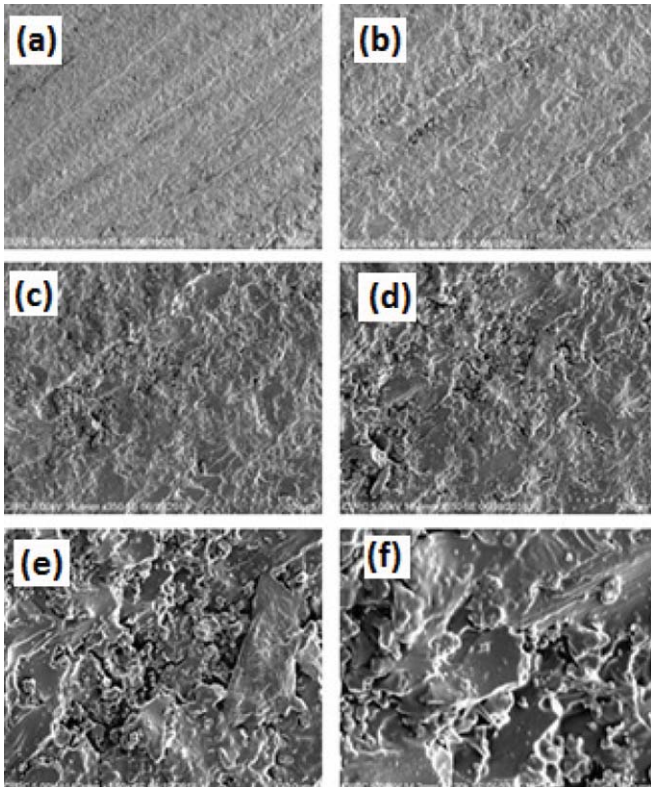


Fig.20: Fractured areas viewed under SEM

on brittle materials have been verified. The specimens' key advantages are their basic test configuration, geometry, and fixtures. The load absorbed by the material before it fails under mode-II is higher than that of mode-I. Specimens offered increased material resistance for mode II dominant loading. The fracture patterns appeared smooth features and with further magnifications courses and striations are also noted indicating the cleavage fracture. The test results and the estimates are considered to be in good agreement.

References

- [1] M. R. Ayatollahi, M. R. M. Aliha, and H. Saghafi, (2011): "An improved semi-circular bend specimen for investigating mixed-mode brittle fracture," *Eng. Fract. Mech.*, vol.78, no.1, pp.110–123, doi: 10.1016/j.engfracmech. 2010.10.001.
- [2] M. R. Ayatollahi, M. R. M. Aliha, and M. M. Hassani, (2006): "Mixed mode brittle fracture in PMMA - An experimental study using SCB specimens," *Mater. Sci. Eng. A*, vol.417, no.1–2, pp.348–356, doi: 10.1016/j.msea. 2005.11.002.
- [3] M. R. M. Aliha, A. Bahmani, and S. Akhondi, (2016): "Mixed mode fracture toughness testing of PMMA with different three-point bend type specimens," *Eur. J. Mech. A/Solids*, vol.58, no. October, pp. 148–162, doi: 10.1016/j.euromechsol.2016.01.012.
- [4] M. Engineering, (2013): "Rock fracture toughness testing using SCB specimen M. R. Ayatollahi 1,* , M. J. Alborzi 1 1," pp. 1–7.
- [5] T. Funatsu, N. Shimizu, M. Kuruppu, and K. Matsui, (2014): "Evaluation of Mode I Fracture Toughness Assisted by the Numerical Determination of K-Resistance," *Rock Mech. Rock Eng.*, vol.48, no.1, pp.143–157, doi: 10.1007/s00603-014-0550-8.
- [6] K. V. N. Surendra and K. R. Y. Simha, (2013): "Design and analysis of novel compression fracture specimen with constant form factor: Edge cracked semicircular disk (ECSD)," *Eng. Fract. Mech.*, vol.102, pp.235–248, doi: 10.1016/j.engfracmech.2013.02.014.
- [7] K.V.N. Surendra and K.R.Y. Simha, (2014): "Analysis of cracked and un-cracked semicircular rings under symmetric loading," *Eng. Fract. Mech.*, vol. 128, no. C, pp. 69-90, doi: 10.1016/j.engfracmech. 2014.07.004.
- [8] M. R. Ayatollahi and S. Pirmohammad, (2013): "Experimental determination of mode II fracture resistance in asphalt concretes," 13th Int. Conf. Fract. 2013, ICF 2013, vol. 7, pp. 5947–5954.
- [9] K. V.N. Surendra and K.R.Y. Simha, (2013): "Synthesis and application of weight function for edge cracked semicircular disk (ECSD)," *Eng. Fract. Mech.*, vol. 107, pp. 61-79, doi: 10.1016/j.engfracmech. 2013.05.010.
- [10] S. Devalapur and H. V Lakshminarayana, (2014): "Studies on Mixed Mode Fracture: Prediction and Verification," *Int. J. Mech. Ind. Technol.* ISSN, vol.2, no.1, pp.130–137.